High Voltage Cable Shield Voltage Monitoring Method Considering Coil Flux

Qiu-jiao Huang(✉) and Dan-kang He

Guangxi Modern Polytechnic College, Hechi 547000, China
huangqiujiao3259@163.com

Abstract. The traditional high-voltage cable shielding layer voltage monitoring method adopts the phase comparison method, which is easy to be interfered by external electrostatic induction, magnetostatic induction and other factors, resulting in low monitoring accuracy and efficiency. In view of the above problems, this paper studies the high-voltage cable shielding layer voltage monitoring method considering coil magnetic flux. After calculating the transfer impedance of cable shielding layer, the calculation model of high voltage cable magnetic flux mutual inductance parameters is constructed. The parameters such as induced voltage of cable shielding layer are determined, and the collected voltage signal is processed by morphology. Using Duffing chaos detection principle, the shielding layer voltage monitoring results are obtained. The experimental results show that the proposed method has high monitoring efficiency, and the minimum effective monitoring rate is 94.3%.

Keywords: Coil flux · High voltage cable · Cable shielding layer · Voltage monitoring

1 Introduction

Compared with fossil energy, electric energy has the advantages of easy control and convenient transmission. After the outbreak of the second industrial revolution, electric energy has gradually become the preferred energy for many industrial sectors. High voltage cable is an important part of power transmission, high-voltage cable transmission power, causing a greater transmission burden to the cable. Therefore, the high-voltage cable is composed of multi-layer structure, and the shielding layer is a layer of metal material on the surface of the cable and connector, which can ensure the normal operation of the cable [1–3]. In general, the shielding layer of high-voltage cable is used to balance the unbalanced current generated by three-phase alternating current, meet the short-circuit current requirements of single-phase grounding fault when the cable is running, and protect the high-voltage cable from the effect of electric force under the changing unbalanced magnetic field, so that the power cable terminal is under the effect of mechanical force caused by electric force for a long time, especially for the stress area of the cable terminal, it is easier to cause damage, leading to electrical insulation damage and shortening the service life of the cable terminal. Monitoring the grounding effect of high-voltage cable shielding layer is an important way to timely pay attention to the safety of high-voltage cable operation. By collecting, transmitting and

S. Wang et al. (Eds.): IoTCare 2021, LNICST 414, pp. 476–491, 2022.
https://doi.org/10.1007/978-3-030-94185-7_32

analyzing the current and voltage signals of cable shielding layer, the state of shielding layer can be obtained in real time to achieve the purpose of safety protection. The traditional high voltage cable shielding layer monitoring method uses hardware data collector to collect the shielding layer status data in the section, and obtains the monitoring results under manual processing. This traditional monitoring method has high requirements for hardware equipment and technical personnel, and it is difficult to ensure more accurate monitoring effect. The online monitoring and signal transmission technology provides the basis and convenience for the intelligent development of power system [4].

In the power system, the usual test method to judge whether the cable insulation shielding layer is good or bad is to apply over-voltage to the tested cable insulation. The common methods include DC withstand voltage and AC withstand voltage to test whether the cable insulation withstand voltage passes or not, and the DC leakage current can also be detected when DC withstand voltage. However, the current intensity of high-voltage cable transmission will be affected by the grid load, and its data monitoring is more complex. Therefore, monitoring voltage is usually used to monitor the working state of high voltage cable shielding layer. The monitoring method based on the dielectric loss method compares the phase of the signal obtained on all monitoring cables with the voltage signal on the bus to monitor the dielectric loss factor of all cables [5]. This method can reflect the overall situation of the shielding layer, but the external interference factors such as serious electrostatic induction, magnetostatic induction and corona discharge with wide spectrum will lead to large monitoring deviation. The high voltage cable shielding layer voltage monitoring method based on LabVIEW virtual instrument for upper computer and lower computer makes use of the high measurement accuracy and powerful function of the data acquisition card provided by LabVlEW, but it is not conducive to the expansion and large-scale application of the monitoring method, and the price is expensive, which is not conducive to cost saving. Based on the above analysis, this paper will study the high voltage cable shield voltage monitoring method considering coil flux.

2 Voltage Monitoring Method of High-Voltage Cable Shielding Layer Considering Coil Magnetic Flux

2.1 Calculation of Transfer Impedance of Cable Shielding Layer

Whether in the time domain or the frequency domain to establish the electromagnetic field coupling model to the shielded cable, it is necessary to know the distribution parameters along the line and the transfer impedance of the shielding layer. Transmission line distribution parameters are the basis for establishing external cable coupling, while transfer impedance is the bridge connecting the internal and external loop couplings. The factors that affect the coupling are the inductance, capacitance, conductance and resistance per unit length, mainly the solution of distributed inductance and distributed capacitance. The solution to the distribution parameters is closely related to the selection of the reference conductor, including one of the transmission lines as the reference conductor, the shielding layer as the reference conductor, and the

ground as the reference conductor. The coupling of a complete shielded cable is divided into internal and external transmission systems. The external transmission system and the internal transmission system use the earth and the shielding layer as reference conductors respectively.

The transverse electromagnetic field structure and the corresponding propagation mode are the basic assumptions of the theoretical analysis of the transmission line. Even if the electromagnetic field changes with time, the voltage and current between the transmission line conductors can still be uniquely defined. The general simplified form of the equation of $n+1$ multi-conductor transmission line is as follows [6]:

$$\begin{aligned} \frac{\partial}{\partial z}V(z,t) &= -RI(z,t) - L\frac{\partial}{\partial z}I(z,t) \\ \frac{\partial}{\partial z}I(z,t) &= -GV(z,t) - C\frac{\partial}{\partial z}V(z,t) \end{aligned} \tag{1}$$

Among them, R and G are the impedance matrix per unit length and the conductance matrix per unit length respectively, which are ignored for lossless conductors.

$$L = \begin{bmatrix} l_{11} & l_{12} & \cdots & l_{1n} \\ l_{21} & l_{22} & \cdots & l_{2n} \\ \vdots & \vdots & \ddots & \vdots \\ l_{n1} & l_{n2} & \cdots & l_{nn} \end{bmatrix} \tag{2}$$

$$C = \begin{bmatrix} \sum\limits_{k=1}^{n} c_{1k} & \cdots & -c_{1m} & \cdots & -c_{1n} \\ \vdots & \ddots & \vdots & \ddots & \vdots \\ -c_{m1} & \cdots & \sum\limits_{k=1}^{n} c_{mk} & \cdots & -c_{mn} \\ \vdots & \ddots & \vdots & \ddots & \vdots \\ -c_{n1} & \cdots & -c_{nm} & \cdots & \sum\limits_{k=1}^{n} c_{mn} \end{bmatrix} \tag{3}$$

The matrices L and C are the distributed inductance matrix and the distributed capacitance matrix, respectively. l_{ji} and l_{ij} are the self-inductance of the i conductor and the mutual inductance of the i conductor and the j conductor, respectively. c_{ii} and c_{ij} are the self-capacitance of the i conductor and the mutual capacitance of the i conductor and the j conductor. Because the mutual inductance and mutual capacitance between the two conductors are equal, $l_{ji} = l_{ij}$, $c_{ii} = c_{ij}$, the inductance matrix and the capacitance matrix are all symmetrical.

First, analyze the basic sub-problem of magnetic flux generated by a wire with a uniformly distributed current I. For the transverse electromagnetic field, using the Ampere's law loop, assuming that the circular magnetic field at the same distance from the center of the wire is of the same size, the area along the circumference of the

distance r is divided, and the magnetic flux per unit length can be obtained as follows [7]:

$$\begin{aligned} \int_I Hdl &= I \\ H_\varphi &= \frac{I}{2\pi r} \\ \psi &= \frac{\mu I}{2\pi}\ln\left(\frac{r_2}{r_1}\right) \end{aligned} \tag{4}$$

In the above formula, H is the magnetic flux; l is the current component; I is the wire current; H_φ is the cross-sectional magnetic flux of the wire; r_1 and r_2 are the distance between the wire and the magnetic flux surface. In the same way, the entire magnetic flux wire can be obtained.

When the spacing of the high-voltage transmission line is wide, the dielectric insulating layer of the transmission line only slightly changes the capacitance distribution around the wire. If the surrounding medium is considered to be uniform, the inductance matrix and the capacitance matrix have the following important relationship [8]:

$$LC = CL = \mu\varepsilon A \tag{5}$$

In the formula, μ and ε are the permeability and permittivity of the medium surrounding the conductor, and A is the identity matrix. Through the obtained unit distribution inductance matrix, the unit capacitance matrix can be calculated.

For shielded cables with the shielding layer as the reference conductor, the inner shielding layer is a multi-conductor transmission line. The radius of the shielding layer is r_{SH}, and the distance between the wire i and the wire j from the center of the shielding layer axis is the angle formed by d_i and d_j as θ_{ij}. Similar to the ground plane as the reference conductor, replace the shielding layer with mirrored wires.

It can be obtained from inductance and mutual inductance as [9]:

$$\begin{aligned} l_{ii} &= \frac{\mu_0}{2\pi}\ln\left(\frac{r_S^2 - d_i^2}{r_S r_i}\right) \\ l_{ij} &= \frac{\mu_0}{2\pi}\ln\left[\frac{d_j}{r_S}\sqrt{\frac{\left(d_i d_j\right)^2 + r_S^4 - 2d_i d_j r_S^2\cos\theta_{ij}}{\left(d_i d_j\right)^2 + r_S^4 - 2d_i d_j^3\cos\theta_{ij}}}\right] \end{aligned} \tag{6}$$

Find the distributed capacitance matrix through the relationship between L and C.

Braided shielding layer is widely used due to its good shielding effect. For high frequency electromagnetic interference, a braided shielding sheath with high coverage is generally used. However, as the frequency increases, electromagnetic energy will be coupled into the inside of the sheath through the woven mesh, and it will also cause certain interference to the cables inside the sheath. Therefore, the transfer impedance is

used to indirectly measure the shielding performance of the shielding layer. The smaller the transfer impedance, the better the shielding performance, and vice versa.

The braided layer of the braided shielding sheath is generally copper tinned material. The weaving bundles of opposite directions are cross-knitted in and out to form many tiny diamond-shaped holes, which saves materials and prevents the weaving coverage rate from reaching 100%. The method of solving the transfer impedance of the shielded cable layer is to analyze the coupling mechanism of the external electromagnetic field to the braided shielding layer, and then further derive the calculation formula. The most basic braiding parameters are as follows: (1) the inner diameter of the shielding layer D_0; (2) the number of braided cross strands per unit length p; (3) the number of braided strands c; (4) the number of wires per share N; 5) The diameter d of each braided thin wire (Fig. 1).

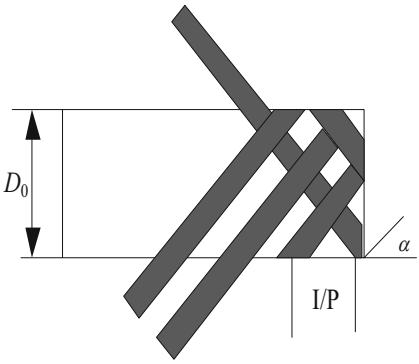

Fig. 1. Side development view of braided shielding layer

Analyze the coupling mechanism of the electromagnetic field on the braid. When the external time-varying electromagnetic field is irradiated on the braided layer with incomplete coverage, scattering, transmission and diffraction will occur on the shielding layer.

According to the theoretical analysis of electromagnetic field, the transfer impedance formula of braided cable is as follows [10]:

$$Z_t = Z_d + (M_h + M_b) \tag{7}$$

In the formula, Z_d means that the transient electromagnetic field will produce scattering characteristics when radiating onto the braided layer, which is a good representation of its low-frequency characteristics, and it will drop rapidly as the frequency increases. M_h is the small hole inductance caused by the transmission of the magnetic field through the mesh of the braid. M_b is the braided inductance generated by the cross braiding of braided bundles and the magnetic lines of force in the gap between the braided bundles. These three parts together constitute the transfer impedance of the braided shielding layer.

Table 1 below shows the relationship between the number of braided strands and coverage [11].

Table 1. The relationship between the number of braided strands and coverage

Number of shares N	Inner diameter of shielding layer D_0	Braided corner /°	d	C	Thickness of braid coverage %
6	4.8	20	0.15	16	71.33
6	4.8	20	0.15	18	77.21
6	4.8	20	0.15	20	82.42
6	4.8	20	0.15	22	86.95
6	4.8	20	0.15	24	90.81

At present, the most used and theoretically accurate calculation formula for scattering impedance is derived from the research of Vance, which characterizes the low-frequency characteristics of electromagnetic field scattering to the braid. After calculating the transfer impedance of the cable shielding layer according to the above process, a calculation model for the magnetic flux mutual inductance parameters of the high-voltage cable is constructed.

2.2 Construction of Calculation Model for Magnetic Flux Mutual Inductance Parameters of High-Voltage Cables

Unbalanced three-phase currents, unequal lengths of cross-interconnected segments, asymmetrical geometric arrangement, etc. will all cause the sheath current to increase. The sheath impedance is greater than the conductor impedance, and the additional temperature rise caused by the heating of the sheath current will reduce the current carrying capacity of the cable and increase the temperature of the cable. When the outer sheath is damaged, it may even cause thermal breakdown of the cable. Therefore, the magnetic flux mutual inductance parameters of high-voltage cables are calculated by constructing a model.

The defined average diameter d_s (unit: m) of the sheath of the shielding layer is shown in the following formula.

$$d_s = \frac{d_{se} + d_{si}}{2} \tag{8}$$

Among them, d_{se} is the outer diameter of the corrugated sheath, and d_{si} is the inner diameter of the corrugated sheath. To calculate the mutual inductance of the sheath, the upper and lower limits of the integral need to be determined, that is, the thickness t_s of the sheath needs to be considered. For the convenience of comparison, this paper uses the geometric mean radius (equivalent radius) to calculate the mutual inductance of the cable, and the approximate solution obtained is consistent with the equivalent diameter

method. Assuming the equivalent radius, the protective layer can be equivalent to a hollow cylinder with an inner radius of $r_s - 0.5t_s$ and an outer radius of $r_s + 0.5t_s$.

According to Biot-Savart's law, the magnetic induction intensity B (unit: T) generated by the core current I at a distance from the wire r is:

$$B = \frac{\mu_0}{4\pi} \int_{\theta_1}^{\theta_2} \frac{I \sin\theta d\theta}{r} \tag{9}$$

Among them, θ_1 and θ_2 respectively fix the angle between the first and last ends of the straight wire and the line at ρ and the current element. When the core is long enough, $\theta_2 = \theta_1 \approx \pi/2$.

According to Gauss's theorem, the magnetic flux Φ (unit: Wb) passing through the sheath is equal to the area fraction of the magnetic induction intensity vector B generated by the core current to the section S of the sheath:

$$\Phi = \iint_S B \cdot dS \tag{10}$$

The mutual inductance M (unit: H/m) between the core and the sheath of the high-voltage cable of length z can be obtained according to Faraday's law of electromagnetic induction [12, 13]:

$$M = \frac{\Phi}{I} = \frac{\mu_0}{2\pi} \iint_S \frac{z}{r} dS \tag{11}$$

Among them, S is the position between the outer edge of the wire core and the center line of the metal sheath.

Currently, there are three manufacturing processes for corrugated sheaths: extrusion, hydrogen arc welding, and embossing. The embossing shape of the sheath mainly has three types: threaded, ring-shaped and smooth, of which the threaded shape is the most common. The inner and outer surfaces of the thread-shaped sheath are curved helical surfaces formed by the spiral motion of a curve (press roller or pressing wheel), and the thickness of the sheath remains unchanged. The threaded cable moves at a uniform speed along the axis, and the pressure roller or pressure wheel continues to be extruded. The movement pitch distance of the ring-shaped cable is squeezed by the pressure roller or the pressure wheel once. The sheath of the smooth sheathed cable does not need to be squeezed, and can be equivalent to a coaxial cylinder.

For corrugated (threaded and ring-shaped) metal sheathed high-voltage cables, the cross-sectional geometry of the magnetic line of force and the sheath is different from the smooth sheath. When the corrugated metal sheath formula (11) is used to calculate the mutual inductance of cables, the geometric shape of the sheath corrugation needs to be considered to determine the integral boundary conditions and solve the analytical solution of mutual inductance. In this paper, the parameter equations of the ring-shaped and spiral-shaped corrugated sheaths are established as the boundary conditions of Eq. (11), and the analytical solution of the mutual inductance of the ring-shaped and threaded sheathed cables is derived. Through the projection of the shielding layer, the

corresponding structural parameter equation of the shielding layer is established. According to the structure parameter equation of the shielding layer, the calculation model of the magnetic flux of different cable shielding layers in the electric field can be obtained. After the above-mentioned cable magnetic flux mutual inductance parameter model is established, the induced voltage of the cable shielding layer is calculated.

2.3 Calculation of Induced Voltage on Cable Shield

For single-core cables, the induced voltage of the metal sheath is completely different from that of three-core cables. The induced voltage on the metal sheath of a single-core cable depends on the load current of the cable and the arrangement and line length of the cables in the same circuit, as well as the arrangement and distance of the surrounding circuits. The relationship between the conductor and the metal sheath of a single-core cable can be regarded as the primary winding and secondary winding of a transformer. When the cable wire passes current, magnetic flux is generated around it. The magnetic flux is not only connected to the core loop, but also connected to the metal sheath of the cable, and induced voltages are generated on the core and the metal sheath respectively. Since each core has a dedicated metal protective layer, the magnetic flux generated by the load current or short-circuit current is interlinked with the metal protective layer, so there is always an induced voltage on the metal protective layer. The value of this induced voltage is related to the cross-section of the core, the distance between the cables and the current and the length of the cable. Especially when the cable is very long, the induced voltage on the sheath can reach a higher value.

In Fig. 2, p represents the metal sheath of the single-core cable, which can be regarded as a conductor parallel to the three-phase cores A, B, and C. The distance between the centers of the four conductors is expressed as a ratio, that is, the center distances between the cores AB, BC, and CA are S, mS, and nS; the center distances between the conductor p and the cores A, B, and C are respectively D, βD, and αD.

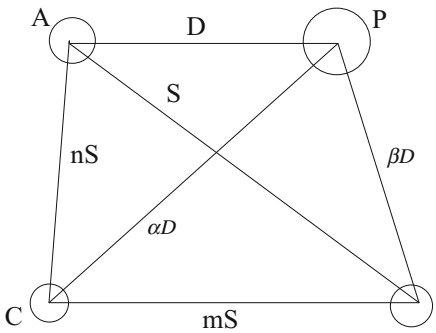

Fig. 2. Representation of the center distance between the metal sheaths of a single-core cable

According to the above analysis, it can be seen that there is an induced electric potential in the metal sheath, and the metal sheath connects the cross interconnection to

protect the ground to form a loop with the earth. Circulating current will be generated when the three-phase grounding is unbalanced due to grounding methods, grounding defects, and grounding faults caused by metal sheath defects. Because this current is generated by the induced potential of the metal sheath acting on the ground loop, it is called this current It is grounding induction circulating current.

Based on the above capacitance parameters, the power cable in operation will generate capacitance current. When one end of the metal shield is grounded, the ground capacitance current and leakage current of the cable have a path. Under normal circumstances, the capacitor current is very small.

When the single-core cable is laid straight and parallel, the equivalent circuit diagram of the metal sheath normally grounded is shown in Fig. 3.

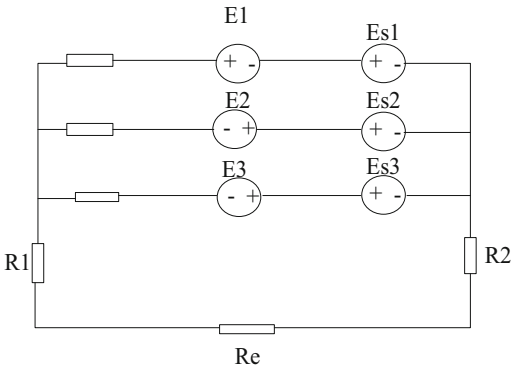

Fig. 3. Equivalent circuit diagram of metal protective layer grounding

E_1, E_2, and E_3 are the unit induced potentials of the metal shielding layer of the three-phase cable due to the main current of the respective cores; E_{s1}, E_{s2}, and E_{s3} are the unit inductions of the metal shielding layer of the two-phase cable to the other phase of the shielding layer. Electric potential; R_1, R_2 are the grounding resistance of the cable metal shielding layer; R_e is the earth resistance (including the leakage resistance of the cable to the earth R_g); R is the cable metal shielding layer resistance; X is the self-inductance of the cable metal shielding layer; X_1 is the unit length The mutual inductance of the metal shielding layer of the middle-phase and side-phase cables; X_2 is the mutual inductance of the metal shielding layer of the side-phase and side-phase cables per unit length.

Through the above derivation, the general calculation formula of the induced voltage of each phase of the cable is obtained, but it is far from enough for the study of the sheath induced voltage, because the above formula does not show the relationship between the induced voltage and the grounding resistance, whether the core transposes or not, and the number of cross interconnection points. When the length of the line exceeds 1000 m, the cable cross interconnection grounding mode is generally adopted, and this mode can also be subdivided into the metal sheath cross interconnection grounding mode and the metal sheath cross interconnection mode, and the wire core is

transposed at the same time. For the convenience of description, these two grounding modes are referred to as semi transposition grounding mode and full transposition grounding mode respectively. According to the relevant simulation research, whether in the horizontal arrangement or the zigzag arrangement, the sheath induced voltage is negatively correlated with the number of cross interconnection points, and is always positively correlated with the distance. However, in the actual cable laying, the smaller the distance is, the better. Therefore, the cable diameter, construction conditions and induced voltage limit should be considered comprehensively, choose the best distance.

When the cables are arranged horizontally, try to choose the full transposition grounding method, because the full transposition is compared with the half transposition, the sheath induced voltage value is significantly reduced, and the overall induced voltage of the line is in a balanced state.

When the cables are arranged in a zigzag pattern, the full transposition and semi transposition grounding methods have almost the same induced voltage curve. Because the full transposition has greater construction difficulty in the actual engineering construction, the semi transposition grounding method can be selected when the induced voltage requirement is not high.

When the cable line is grounded through resistance at both ends, there is a certain relationship between the sheath induced voltage and the grounding resistance, and the voltage increases with the increase of resistance. When the cable line is in the cross connected grounding state, the grounding resistance has little effect on the induced voltage. After determining the quantization process of the above factors affecting the voltage of the cable shielding layer, the voltage signal collected from the voltage data is processed.

2.4 Shield Voltage Signal Processing

After the collected high-voltage cable shielding layer voltage signal undergoes preliminary processing by the hardware part, the signal image is obtained, and the shielding layer voltage signal is processed according to the morphological theory.

The working principle of mathematical morphology is to use structural elements to do morphological operations on the areas that need filtering to filter and analyze the graphics and signals. The parameters of structural elements such as length, shape and the selected morphological operations determine the final filtering results. Because most of the images in real life and the main research are not binary images, but gray images with pixel gray values greater than two, the gray morphology is also used after the promotion of binary morphology. The signal collected from the power system is one-dimensional signal. Aiming at the gray-scale morphological transformation in the case of one-dimensional discrete, there is a new definition of corrosion and expansion operation. The maximum and minimum operation can be used to replace the intersection and union operation in the corrosion and expansion operation defined in the binary image.

Assuming that the input signal $f(n)$ is a discrete function defined on $F = (0, 1, \cdots, N-1)$, and the structural element sequence $g(n)$ is defined as a discrete function on $G = (0, 1, \cdots, M-1)$, and $N \geq M$, the newly defined corrosion expansion operation is as follows:

$$\begin{aligned}(f\Theta g) &= \min(f(n+m) - g(m)) \\ (f \oplus g) &= \max(f(n+m) + g(m))\end{aligned} \tag{12}$$

The corrosion using the new definition of formula (12) is actually an operation to take a minimum value, while the expansion using the new definition of formula (12) is actually an operation to take a maximum value. In the same way, more complex morphological operations can be derived from the two basic operations of grayscale corrosion and expansion operations. Mathematical morphology operation is simple, mainly composed of four basic operations: expansion, corrosion, opening operation and closing operation, which can quickly process and analyze the input signal.

When using a mathematical morphological filter to filter a sampled signal, in addition to the selected mathematical morphology algorithm, the other factor that affects the filtering effect is the selection of structural elements. The selection of structural element parameters mainly includes two aspects: one is the shape of structural elements. Common shapes include straight lines, semicircles, cosines, triangles, etc. The second is the size of the corresponding structural element shape. Structural elements of different shapes and sizes will produce different filtering effects even if they are combined with the same filtering algorithm.

According to the research of experts and scholars at home and abroad in recent decades, the semicircular structural element has the best performance in filtering white noise, the triangular structural element has the best performance in filtering positive and negative impulse noise, and the linear structural element has strong comprehensive denoising ability, which is suitable for processing signals with high transient component content.

In engineering practice, the collected signal is more complex, including many different kinds of noise, so the more structural elements, the better filtering effect will be. But on the other hand, the amount of calculation and the delay are proportional to the shape, size and complexity of structural elements. In order to give consideration to both the filtering effect and the amount of calculation, the following two principles should be followed when designing the parameters of the filter: firstly, when selecting the size of the structural elements, the selected size should not be too long, and should be as short as possible to reduce the workload. Generally, the length of the selected structural elements is between 1/50 and 1/20 of the signal cycle length; Secondly, when selecting the shape of structural elements, we should select the structural elements similar to the shape of the signal to be filtered.

The working environment of power grid is complex, and the sampled power signals are often mixed with many different types of noise. When morphological filters use different shapes of structural elements, the filtering performance will be different. Each shape of morphological filter has its own characteristics, which is suitable for filtering different characteristics of noise. In order to remove all kinds of interference signals more effectively, this paper uses a composite morphological filter, which is composed of basic structural elements with different shapes, and uses the new structural elements to filter and analyze the signals. In this paper, the triangle structure element which has the best performance in filtering positive and negative impulse noise and the sine structure element which is most similar to the waveform of power signal are combined

to form a new morphological filter, which can also play a good filtering effect on the signal disturbed by complex noise.

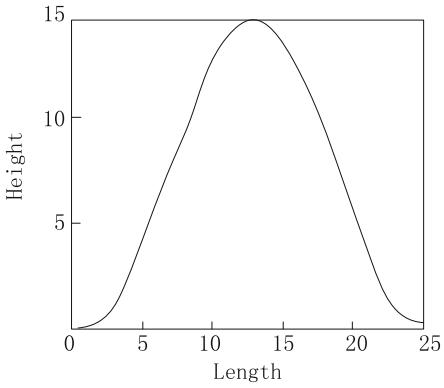

a) Structural elements with a sine shape

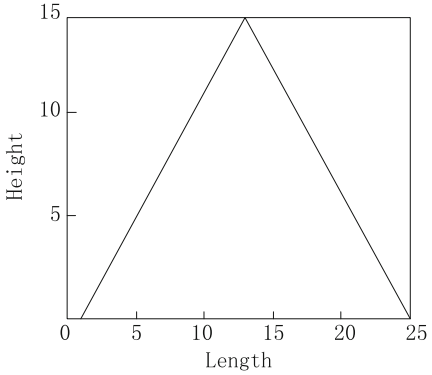

b) Structural elements shaped as triangles

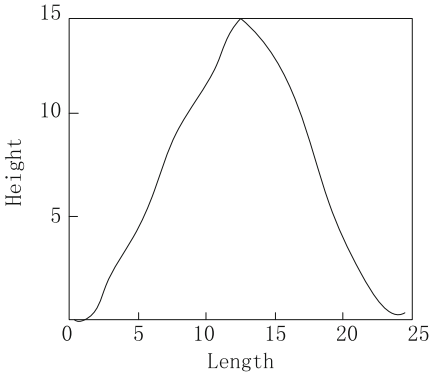

c) Composite structural elements

Fig. 4. Working principle of complex morphological filter

Figure 4a) is a sine-shaped structural element, Fig. 4b) is a triangular-shaped structural element, and Fig. 4c) is a new structural element composed of the above two structural elements. After processing the voltage signal of the shielding layer by using the compound morphological filter of the above structure, the chaos theory is used to realize the voltage monitoring of the shielding layer.

2.5 Realize Shield Voltage Monitoring

After continuous research on the Doffing equation, it is found that the Doffing system can express various properties through its dynamic behavior. The nonlinear dynamic system expressed by the Doffing system has a variety of nonlinear dynamic characteristics, including various complex dynamics such as oscillation, chaos, and bifurcation. This has also become one of the commonly used models for chaos research. The buffing chaotic oscillator equation is a nonlinear vibration system with nonlinear restoring force, and the form is as follows:

$$\ddot{x}(t) + k\dot{x}(t) - x(t) + x^3(t) = a\cos\omega t \tag{13}$$

Among them, k is the damping ratio; ω is the angular frequency of the periodic external force; a is the amplitude of the periodic external force. According to related research:

1) The amplitude of periodic external force affects the trajectory and mode of chaotic motion. Under the same periodic external force frequency, when the amplitude of the periodic external force changes, the dynamic behavior will also change, and the specific manifestation is that the phase trajectory produced by the chaotic motion will also change.
2) The damping coefficient of the system will also affect the threshold of chaotic motion. At the same frequency, when the damping ratio increases, the periodic external force amplitude a that causes chaotic motion will also increase, and its frequency range will also increase. But if the damping ratio is too large, it will cause the chaotic motion to change to a periodic motion.
3) Through the analysis of the phase trajectory changes of the system, it can be explained that the dynamic behavior in the chaotic system is very sensitive to the initial parameters. Therefore, according to the characteristics of the system's dynamic behavior from the chaotic critical state to the phase trajectory of the large-scale periodic state, the detection of the weak signal to be measured is carried out. This is also a practical method of applying the Duffing chaotic system to the theory of detecting weak periodic signals.

The model of using Duffing chaos to detect periodic signals is as follows:

$$\ddot{x} - x^3 + x^5 + k\dot{x} = \gamma\cos\omega \tag{14}$$

Among them, k is the damping ratio; $-x^3 + x^5$ is the nonlinear restoring force of the system; $\gamma \cos \omega t$ is the applied periodic force of the system. The basic idea of using this Duffing chaotic oscillator for periodic signal detection is: first adjust the system parameter γ to reach the critical point γ_0, so that the system is in the state of the boundary between the chaotic state and the large periodic motion state, and then use this signal to be detected as the period of the system's periodic external force. Perturbation is based on the phase change between the chaotic state and the ordered state of the system, and then determines whether the signal to be measured appears, and then adjusts the relevant parameters to achieve the purpose of signal measurement. The motion state of the system can be characterized by the maximum Lyapunov exponent λ of the system. When λ is greater than 0, the system must be in a chaotic state, and the greater the value of λ, the deeper the chaotic depth; when λ is less than 0, the system belongs to Ordered system, that is, periodic system or quasi-periodic system.

According to the above-mentioned Duffing chaotic oscillator to discriminate the system state, the voltage state and value of the shielding layer in the current chaotic period can be obtained accordingly. Comparing the output result of the chaotic system with the voltage state of the shielding layer during normal operation, the monitoring result of the shielding layer voltage of the high-voltage cable is obtained. The above has completed the research on the voltage monitoring method of the high-voltage cable shielding layer considering the coil magnetic flux.

3 Experimental Study

This section will verify the feasibility of the high-voltage cable shielding voltage monitoring method that considers the coil magnetic flux.

3.1 Experiment Content

The experiment adopts the form of comparison, using two traditional voltage monitoring methods as Method 1 and Method 2, to verify the feasibility and reliability of the method from the perspective of monitoring error and monitoring response time of the monitoring method. Three monitoring methods are used to monitor the shielding layer voltage of cables in the same power grid, and the actual value is compared with the monitoring value to obtain an effective monitoring rate; the time when the monitoring data change occurs is recorded as the monitoring response time.

3.2 Experimental Result

The experimental results are shown in the following table. Analyze the data in the table and draw the corresponding experimental conclusions (Table 2).

Table 2. Experimental data

Cable number	Method 1		Method 2		Method of this article	
	Effective monitoring rate/%	Monitoring reaction time/ms	Effective monitoring rate/%	Monitoring reaction time/ms	Effective monitoring rate/%	Monitoring reaction time/ms
1	82.2	51.9	88.5	50.3	95.3	29.1
2	81.4	50.5	88.1	50.7	94.4	29.8
3	78.8	46.7	86.8	49.6	95.7	27.9
4	84.6	53.2	86.8	49.8	94.5	27.8
5	85.0	47.4	88.1	49.6	94.8	28.6
6	83.2	51.2	87.7	50.4	95.3	28.2
7	80.7	49.7	88.5	49.5	95.2	28.1
8	79.1	53.3	87.7	49.1	95.1	27.9
9	84.3	49.1	88.4	48.9	95.6	28.6
10	81.7	42.6	86.6	50.2	95.9	29.7

Analysis of the data in the above table shows that the effective monitoring rate of method 1 is lower than 85%, the effective monitoring rate of method 2 is lower than 88.6%, and the lowest effective monitoring rate of this method is 94.3%, indicating that the monitoring accuracy of this method is higher. In terms of reaction time, the average reaction time of the method in this paper is 28.57 ms, the average reaction time of method 1 is 49.56 ms, and the average reaction time of method 2 is 49.81 ms. The method in this paper is lower, indicating that the method is more efficient. That is to say, the high-voltage cable shielding voltage monitoring method that considers the coil magnetic flux studied in this paper has the advantages of high monitoring accuracy and fast speed.

4 Concluding Remarks

The metal shield grounding of high voltage power cable can effectively ensure that the lines and electrical equipment are not damaged and maintain the stable operation of power system. However, the current application of high-voltage power cable metal shield grounding method has not formed a unified standard. If the correct grounding method is not adopted, it will lead to power accidents, which will not only endanger people's lives, but also cause serious disasters to enterprises. The voltage of the shielding layer of high voltage cable can effectively ensure the normal work of the shielding layer. This paper studies the method of monitoring the shielding layer voltage of high voltage cable considering the coil flux. Based on the calculation of transmission impedance of cable shielding layer, the calculation model of magnetic flux mutual inductance parameters of high voltage cable is established. The induced voltage and other parameters of the cable shielding layer are determined, and the collected voltage signal is processed by morphology. Using Duffing chaos detection principle, the monitoring results of shielding layer voltage are obtained. The experimental results show that the voltage monitoring method has the advantages of high precision and strong stability.

Fund Projects. 1. 2020 Guangxi University Young and middle-aged teachers' scientific research basic ability promotion project: Research on classroom teaching dynamic evaluation system based on mobile terminal (2020ky45011).

2. 2016 Guangxi Vocational Education Teaching Reform Project: Study on the Connection of Project Design between Specialized Courses in "Project Teaching" of Applied Electronic Technology Major in Higher Vocational Education, (GXGZJG2016B003)

References

1. Liu, Y., Xia, X., Li, M., et al.: Research on online monitoring system based on locus method of HV power cable. J. Electric Power Sci. Technol. **34**(03), 202–210 (2019)
2. Wei, D., Yuguang, S., Daizong, T., et al.: Online monitoring method for rotor demagnetization fault of permanent magnet synchronous machine based on new type of search coil. Electric Power Autom. Equipment **40**(06), 218–227 (2020)
3. Liu, S., Liu, D., Srivastava, G., Połap, D., Woźniak, M.: Overview and methods of correlation filter algorithms in object tracking. Complex Intell. Syst. **7**(4), 1895–1917 (2020). https://doi.org/10.1007/s40747-020-00161-4
4. Zhao, W., Xia, X., Liu, Y., et al.: Research on online monitoring for HV cable running locus. In: Proceedings of the CSU-EPSA, vol. 31(09), pp. 137–143 (2019)
5. Qi, H., Zhang, B., Huang, J., et al.: Liquid level intelligent detection of high voltage cable porcelain termination using short-time Fourier transform and deep brief networks. China Measurement Testing Technol. **45**(04), 47–52 (2019)
6. Liu, S., Xia, D., Qiu, Q., et al.: Researches on DC instantaneous over current impulse characteristics of flux coupling type pancake coil. Adv. Technol. Electr. Eng. Energy **38**(01), 47–53 (2019)
7. Yin, Z., Ning, Z.: Study on the test method of nondestructive stress test of space truss structure by magnetic flux method. J. Disaster Prevention Mitigation Eng. **40**(05), 803–810 (2020)
8. Liu, S., Li, Z., Zhang, Y., Cheng, X.: Introduction of key problems in long-distance learning and training. Mob. Networks Appl. **24**(1), 1–4 (2019). https://doi.org/10.1007/s11036-018-1136-6
9. Qi, Z., Li, X., Li, P., et al.: Fault detection method for cable joint based on DKPCA. J. Dalian Univ. Technol. **60**(03), 300–305 (2020)
10. Shenghui, L., Xue, B., Henan, D., et al.: Cable incipient fault identification based on stationary wavelet transform and random forest. Adv. Technol. Electr. Eng. Energy **39**(03), 40–48 (2020)
11. Liu, Z., Su, F., Wang, X., et al.: Partial discharge monitoring system based on cable terminal with distributed wireless TEV sensors. Electr. Measur. Instrum. **56**(17), 102–108 (2019)
12. Liu, S., Liu, D., Muhammad, K., Ding, W.: Effective template update mechanism in visual tracking with background clutter. Neurocomputing (2020). https://doi.org/10.1016/j.neucom.2019.12.143
13. Zhou, L., Cao, J., Wang, S., et al.: Comprehensive state evaluation of high voltage cable based on multi-state variables characteristics and variation law. High Voltage Eng. **45**(12), 3954–3963 (2019)